Supplementary Information

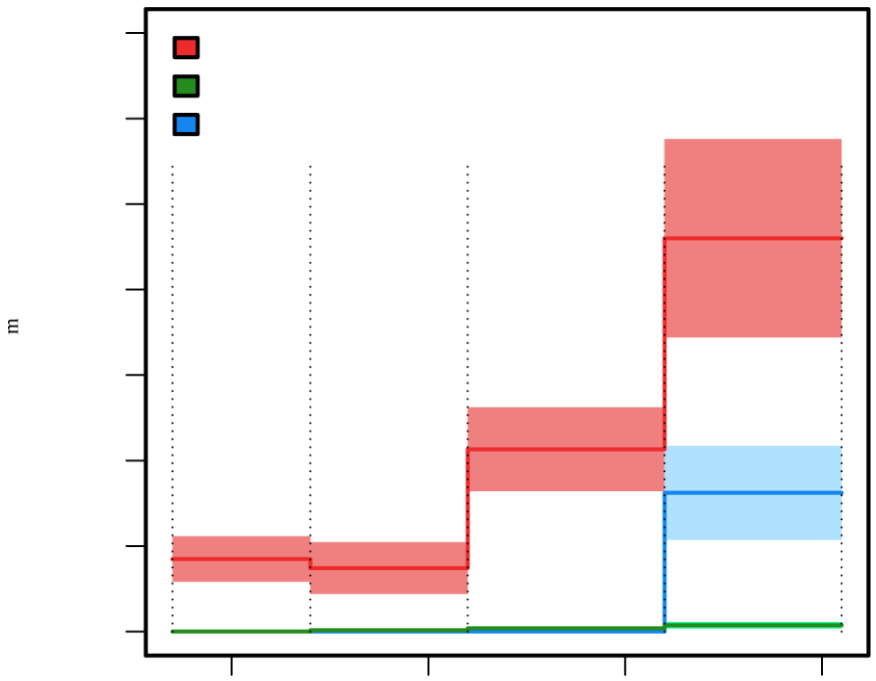

Figure S1. Experimentally determined rates of gonad growth. Shows the total linear growth rate (red), radial growth rate (green) and proximal arm growth rate (blue) for the *C. elegans* gonad over time, according to our measurements. Shaded regions are ±1 s.d.. Growth rates are based on the difference between two length measurements made at the start and end of each developmental phase. The rates shown were used as input parameters to the simulation with some additional processing (for instance, the DTC migration rate is based on the total linear growth, minus any length that can be accounted for by proximal arm elongation).

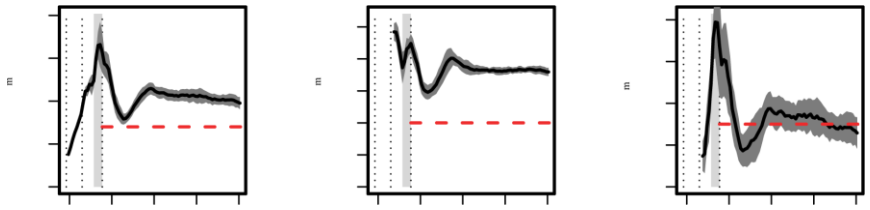

Figure S2. Simulated micron measurements of the proliferative zone. Panel (A) shows the distance from the DTC to the proximal-most cell in mitosis, while (B) shows the distance from the DTC to the distal-most cell in meiosis. (C) shows the length of the meiotic entry region, defined by Hansen *et al*. in 2004 as the region of overlap between proliferative cells and cells in prophase of meiosis I. The simulated lengths in (A) and (B) are longer than the corresponding experimental measurements, particularly just after the model transitions from larval to adult behavior. Together with the fact that simulated cell row counts do match experiment well, this suggests that the effective length of a cell row in the model is slightly too long; either because cells in the real germ line are smaller or because they are under greater compression. The second possibility is more likely, as it is the harder parameter to estimate. However, our main conclusions herein would in fact be strengthened if germ cells are under greater compression than our current model estimates.

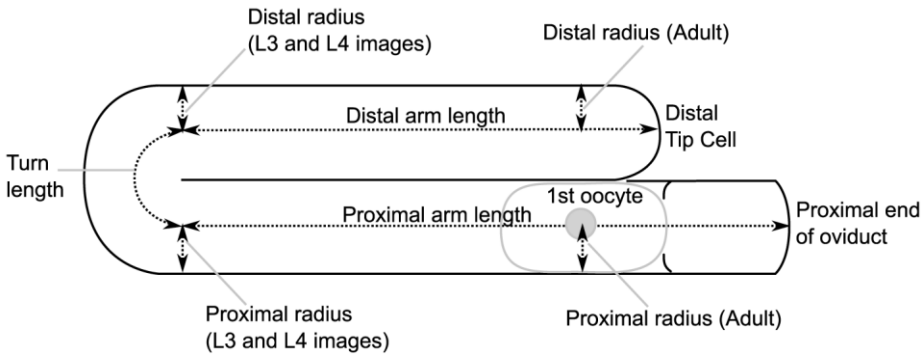

Figure S3. Positions at which DIC microscopy images were measured. Corresponds to the measurements in Table 1. Dotted lines show the paths drawn onto each DIC image and measured using ImageJ.

Figure S4

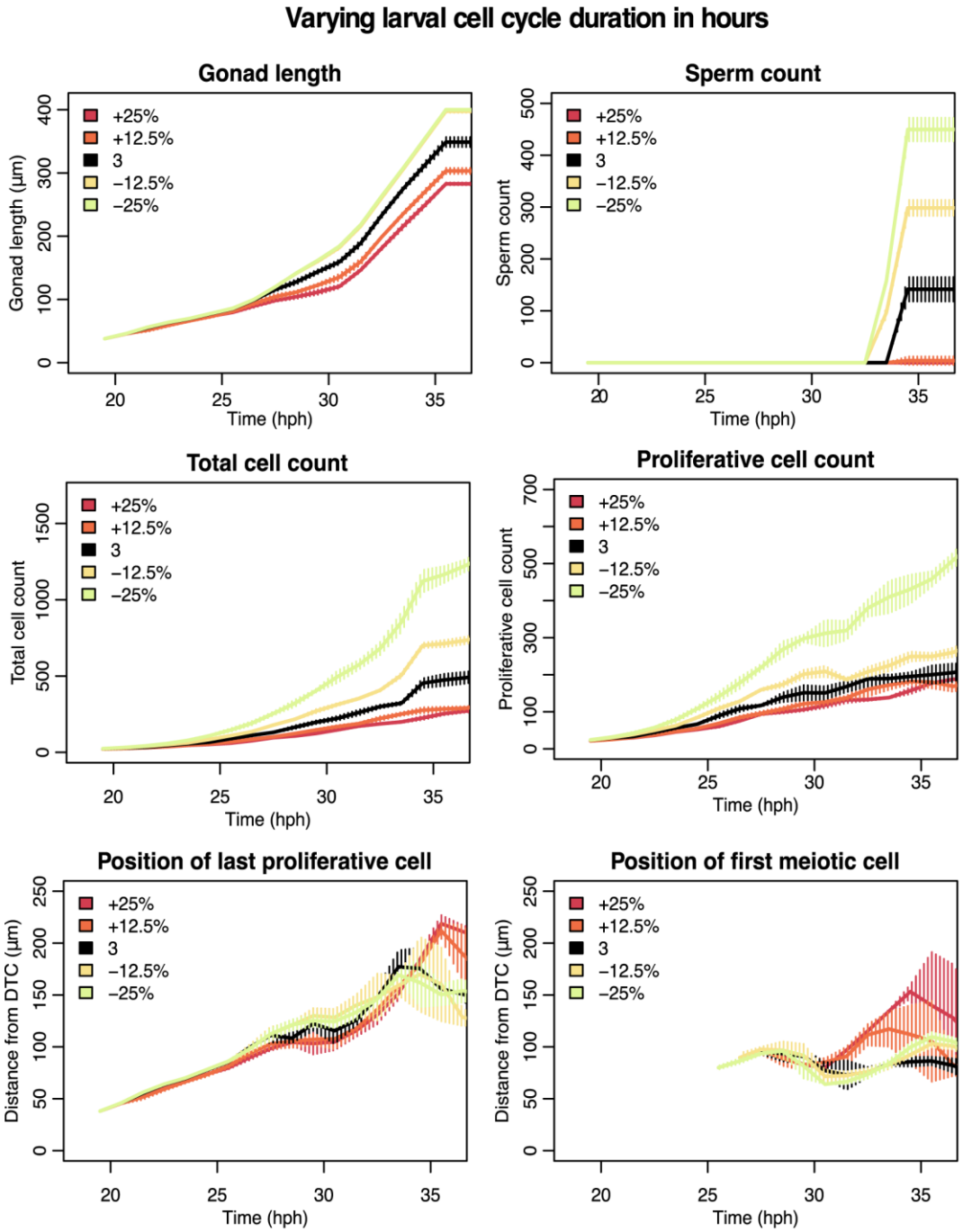

Figure S5

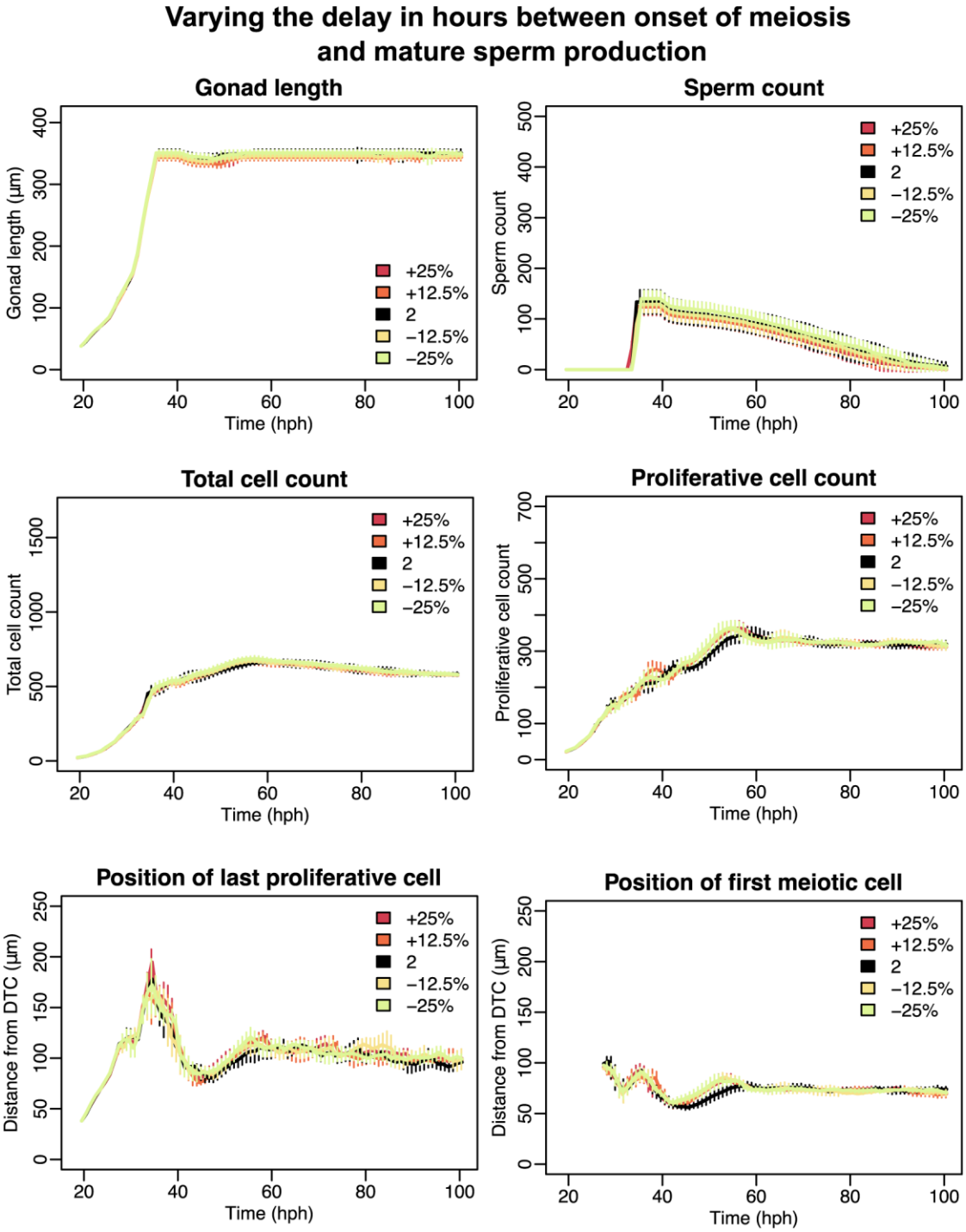

Figure S6

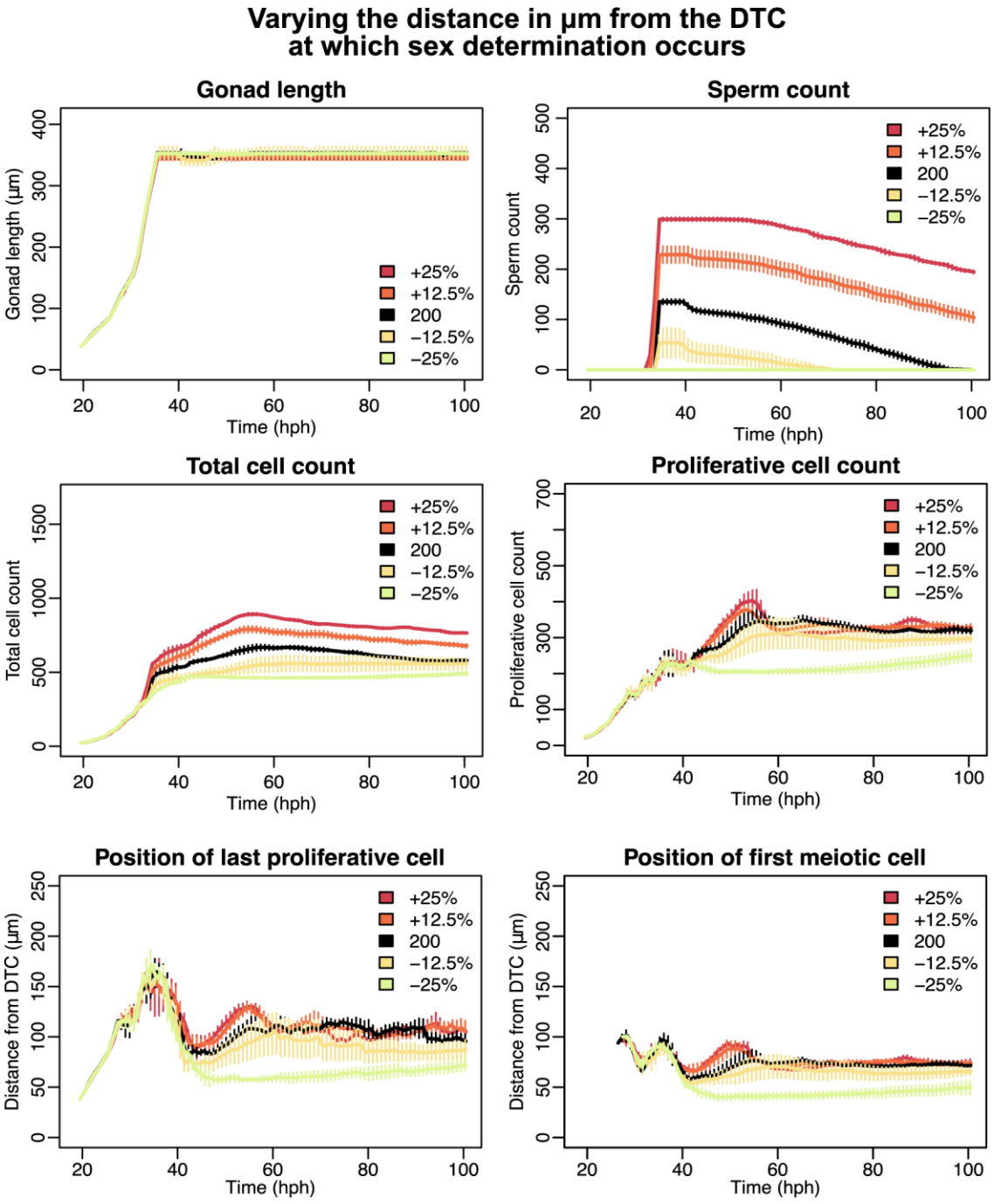

Figure S7

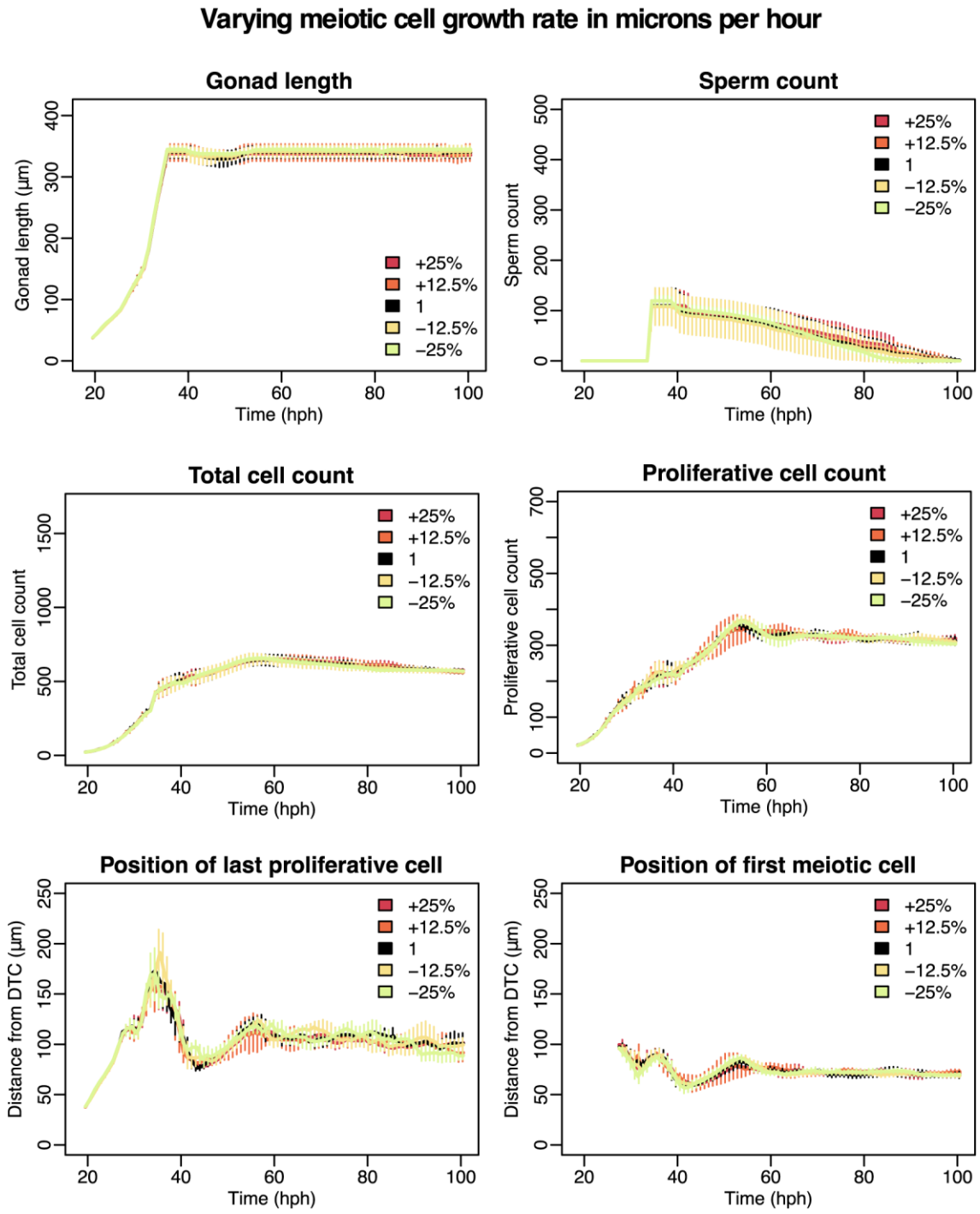

Figure S8

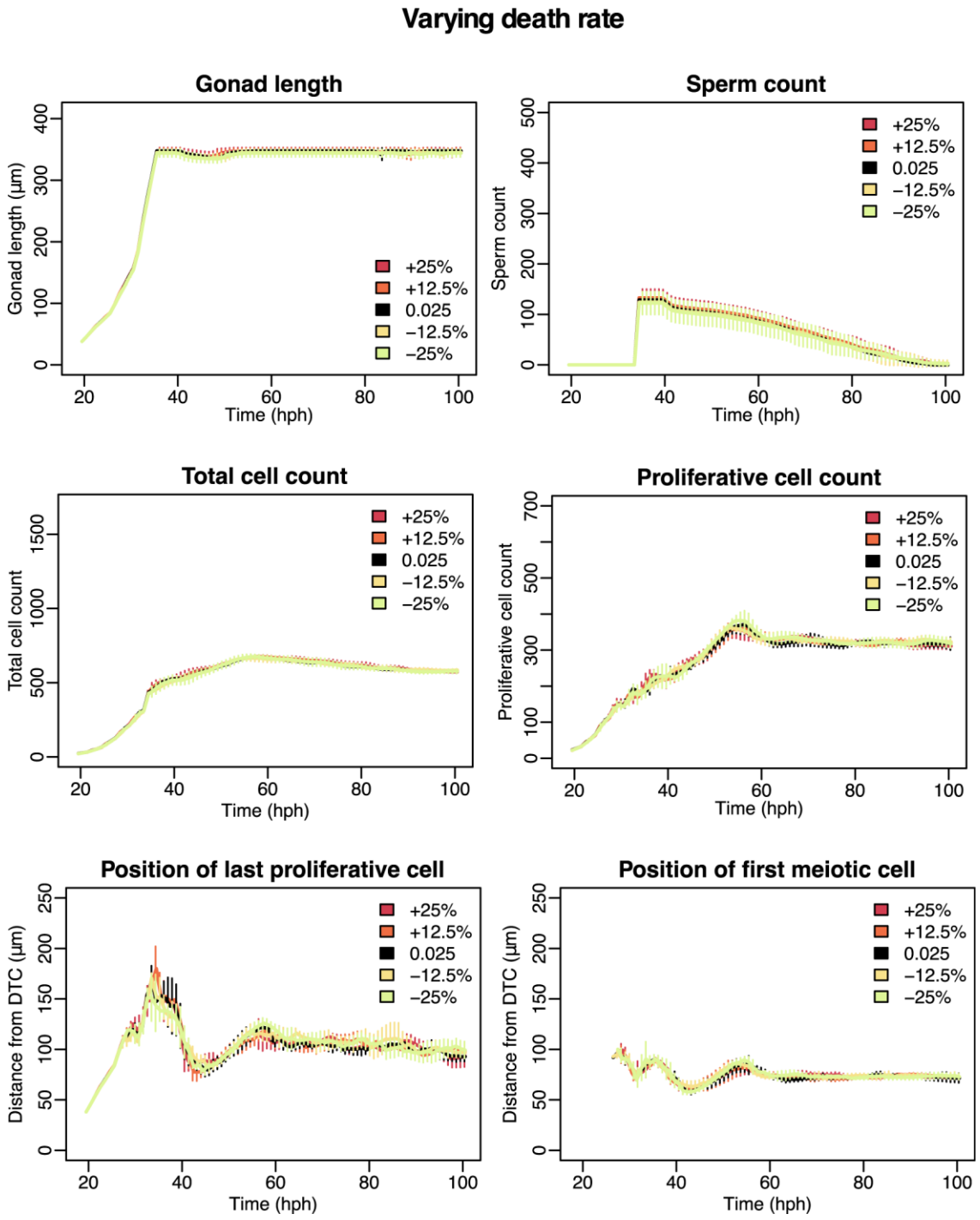

Figure S9

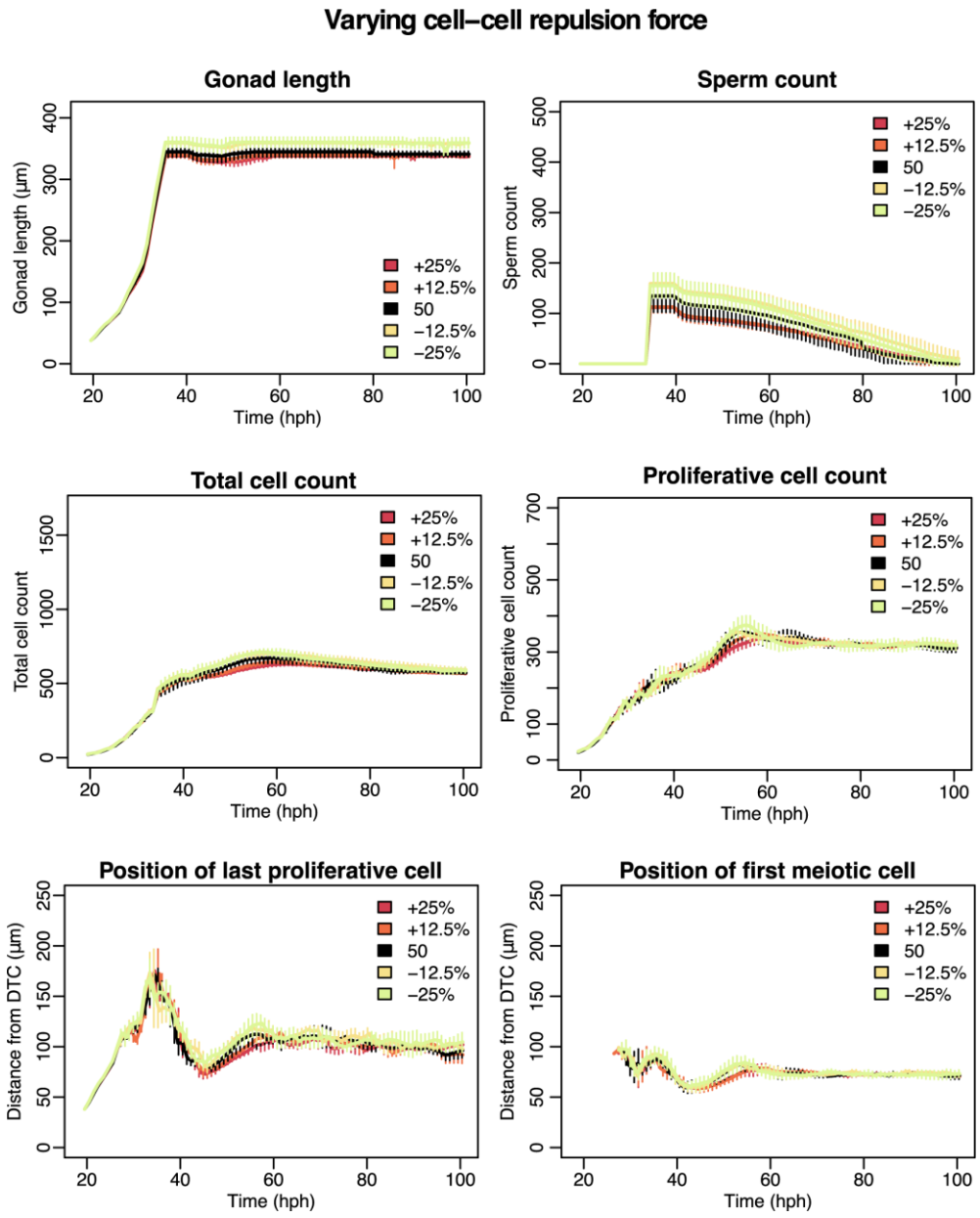

Figures S4-S9. Parameter sweeps showing the effect of a 25% variation in each of the model's free parameters. Free parameters are those that could not be adequately determined from experimental data; these are indicated by a * in Table S1. Supplementary Figures 4-9 show variations in, respectively: larval cell cycle length, delay between meiosis and sperm production, position at which sex determination occurs, meiotic cell growth rate, death rate and cell-cell repulsion strength. Each line is the mean of 5 runs, and the vertically shaded region is ±1 s.d..

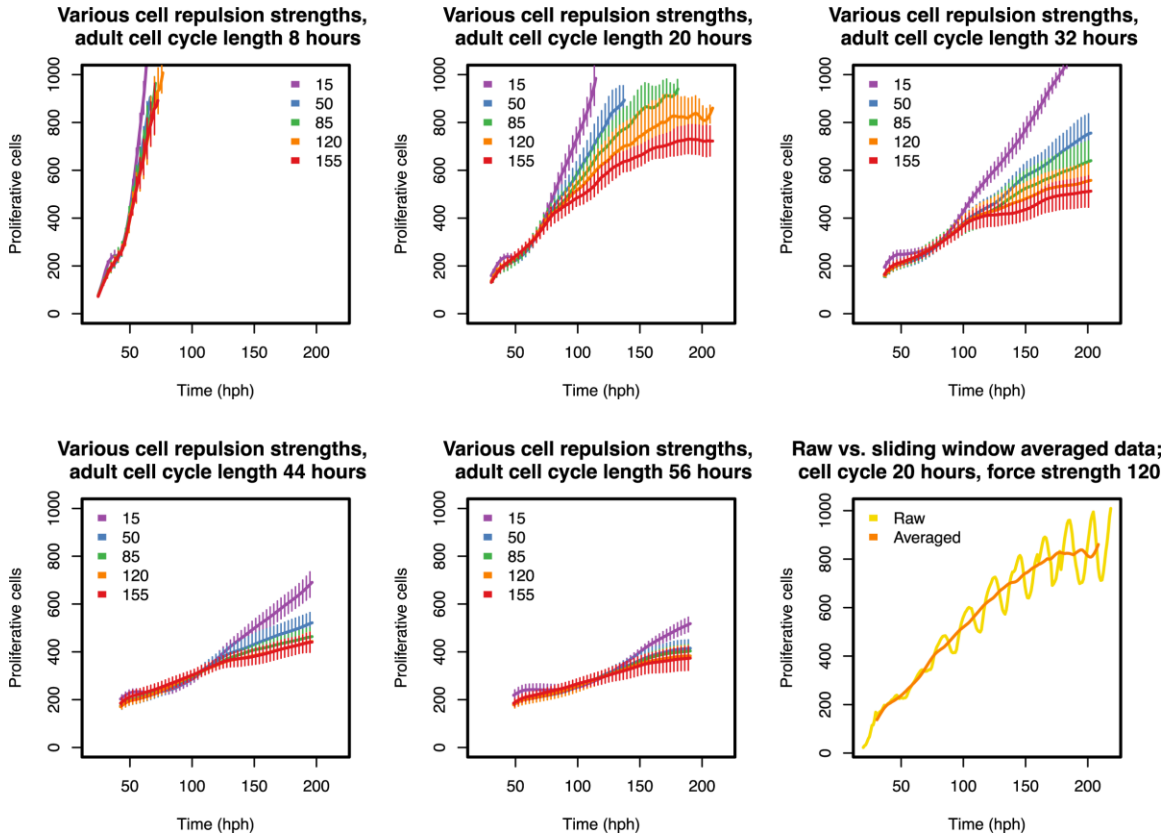

Figure S10. A parameter sweep varying adult cell cycle length and cell-cell repulsion force, in the absence of contact inhibition-like mechanical feedback. A sweep aimed at determining whether a stable proliferative cell count can be maintained without mechanical feedback, by altering the parameter set. For cell cycle lengths in the range 8-24 hrs the proliferative cell count still increased beyond normal levels. Each line is the mean of 5 runs, while the vertically shaded region is ±1 s.d.. Cell counts have been sliding window averaged using a window length equal to half the cell cycle duration, in order to remove phasing and make the general trend more apparent. The final panel compares raw and averaged data for a single choice of parameters.

Table S1. Parameter values and sources. All times are given as hours post-hatching. † From our measurements of microscopy images of the gonad. * Indicates parameters that were tuned to fit the experimental data in Fig. 4. Other parameters were considered fixed based on available data.

Parameter	Value	Reference	Notes
Initial conditions:			
Starting time	18.5 hr	(Wood et al., 1980)	Beginning of L3
Initial germ cell count	16	(Stupay and Hubbard, 2003)	
Initial gonad length	32 µm	(Stupay and Hubbard, 2003)	
Initial gonad radius	5.48 µm/hr	†	
Stretching:			
Rate of stretching growth during late L4	16.2 µm/hr	†	Based on comparing proximal region length at mid L4 and in the adult
Period of stretching growth	31 - 35.5 hr	†	
DTC migration:			
L3 moult - mid L3	8.77 µm/hr	†	Based on change in total gonad length
Mid L3 - L3/L4 moult	7.43 µm/hr	†	Based on change in total gonad length
L3/L4 moult - mid L4	21.3 µm/hr	†	Based on change in total gonad length
Mid L4 - young adult	13.6 µm/hr	†	Change in length – proximal growth
DTC halts	35.5 hr	(Stupay and Hubbard, 2003)	
Radial growth:			
L3 moult - mid L3	0 µm/hr		Our estimate
Mid L3 - L3/L4 moult	0.153 µm/hr	†	Based on average radius measurement
L3/L4 moult - mid L4	0.376 µm/hr	†	Based on average radius measurement
Mid L4 - young adult	0.74 µm/hr	†	Based on average radius measurement
Turning:			
Radius of the turn	11.5 µm	†	Adult proximal & distal arms almost touch

Time at start of turning	23 hr	(Stupay and Hubbard, 2003)	
Cell sizes:			
Mitotic germ cell radius	2.8 µm	†	Our GFP z stacks put this in the 2.5–3.5µm range, taking measurements from both larval and adult images.
Meiotic germ cell radius	4 µm	(Maddox et al., 2005; Nadarajan et al., 2009)	Images in these publications suggest a 3 -5µm range
Oocyte radius	10 µm		Oocytes fill the proximal arm
Sperm radius	1.5 µm	(Shakes et al., 2011)	Based on images in this publication
Cell growth rate	1.0 µm/hr	*	
Force law:			
Baseline drag coefficient η	1	(Dunn et al., 2013)	
Strength of repulsion µ	50	*	
Cell cycle:			
Larval cell cycle duration	3 hr	(Kipreos et al., 1996)*	Compromise between (Kipreos et al., 1996; Lewis and Fleming, 1995)
Adult cell cycle duration	8 hr	(Fox et al., 2011)	
Estimated phase breakdown	2% G1 57% S 39% G2 2% M	(Fox et al., 2011)	
Period over which germ cell cycle length increases	31 – 35.5 hr	(Korta et al., 2012)	After mid L4 but before the adult moult
Other parameters:			
Distance at which GLP1 signal becomes absent	70 µm	(Stupay and Hubbard, 2003)	Approximate position at which the first meiotic cell appears during development
Position at which sex determination occurs	200 µm	*	
Sperm/oocyte switch time	32.5 hr	(Barton and Kimble, 1990)	Approximate end of the *fog-1* temperature sensitive period
Sperm production delay	2 hr	*	
Distance from the DTC at which oocyte growth	250 µm		Just beyond the start of the proximal arm. Allowing

begins			oocyte growth everywhere in the proximal arm results in large cells blocking the turn.
Stochasticity *s*	0.1		Arbitrary, prevents synchronised divisions
Hourly apoptosis probability *p*	0.025	*	Produces sustained ovulation with a reasonable rate

Table S2. Cell counts for a single run. These counts apply to the run depicted in Figure 3 of the main text only.

	Time (hours post-hatching)*							
	18.5	**27.5**	**30.5**	**32.5**	**33.5**	**35.5**	**60.5**	**87.5**
Proliferative + Meiotic S (yellow cells)	16	113	147	184	174	228	366	314
Proliferative - Meiotic S	16	105	112	134	147	177	319	299
Meiotic S	0	8	35	50	27	51	47	15
Meiotic (green cells)	0	8	85	80	76	57	143	178
Sperm/ Spermatogenic (blue cells)	0	0	0	38	38	152	111	47
Oogenic (pink cells)	0	0	0	0	36	69	60	83
Meiotic + Spermatogenic + Oogenic	0	0	0	118	150	278	314	308

*In later time points gametes are lost to fertilization.

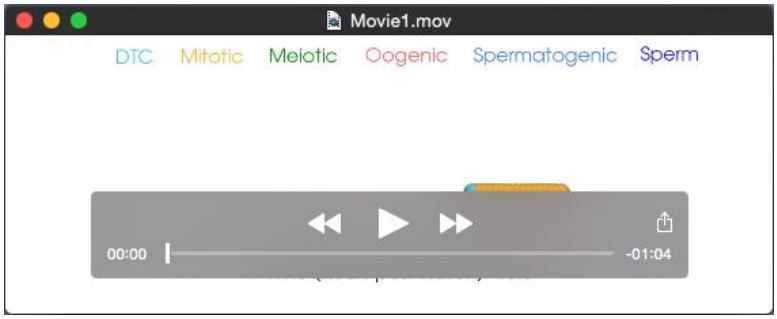

Movie 1. A germline simulation recorded throughout larval development and into adulthood.

Parameters as listed in Table S1.

Supplementary Materials and Methods

This section is intended to further clarify certain details of the computational model, namely: (1) the mathematics of the cell mechanics model, (2) how the boundary condition is implemented, (3) how a statechart updates over time, and (4) how mechanical feedback on the cell cycle is applied.

1) Cell Mechanics

The mechanics simulation uses Chaste, an open source C++ biological modeling library (see Mirams et al., 2013). Each germ cell is represented by a deformable sphere. When cells i and j overlap, cell i experiences a repulsion force given by:

$$F_{ij} = \mu(R_i + R_j)\log\left(1 - \frac{d_{ij}}{(R_i+R_j)}\right)r_{ij}, \quad (1)$$

where r_{ij} is the unit vector from i to j, R_i and R_j are cell radii, d_{ij} is the length of the overlap between the cells, and μ is a spring strength constant. Given the force law in (1), cell positions are updated using forward Euler time stepping and assuming the overdamped form of Newton's second law:

$$\eta\frac{dr}{dt} = F,$$

where η is a drag coefficient and F the net force on the cell found by summing all contributions. As a wide range of cell sizes are present in the germ line, we allow cell size to affect movement by increasing the drag coefficient linearly with cell radius. The final update equation for cell positions is:

$$r_i^{new} = r_i^{old} + dt\left(\frac{\eta R_i}{5}\right)^{-1}\sum_j F_{ij},$$

where η is a drag coefficient appropriate for cells of radius 5 μm (Dunn et al., 2013).

2) Boundary Condition

Germ cells are confined to the gonad by a boundary that updates over time. To capture gonad growth, we explicitly model DTC migration and form a tubular boundary along its path. The DTC migrates in three prescribed stages; first travelling in a straight line along the ventral surface of the worm, turning onto the dorsal surface during the L3/L4 molt, then migrating back into the center of the animal and halting during the adult molt. The DTC's target speed is fixed for each simulation stage, based on our experimental measurements of gonad dimensions. We additionally prescribe that germ cells must be no more than 5 μm (~1 cell diameter) behind the DTC for it to progress. This constraint prevents a biologically unrealistic gap opening up between the DTC and following cells.

As the DTC moves, a collection of equally spaced points on its path is stored, which

defines the organ midline (see panel A below). A small point separation of 2 μm ensures an accurate representation of the curved geometry. At each time step, if a cell is further from the midline than (*gonad radius* – *cell radius*), it lies outside the boundary and is moved toward the midline until it lies just inside again. Cells near the ends of the gonad are subject to a different position correction that generates hemispherical endcaps (see panel A).

Certain details specific to the *C. elegans* gonad are also taken into account in the boundary condition. First, all germ cells in the distal region and turn are forced to lie just inside the boundary, forming a monolayer. An empty space representing the rachis is thereby created in the center of the organ. Second, our experimental measurements showed that the proximal gonad lengthens during L4, an effect that cannot be captured by moving the DTC. To reflect this, points on the midline of the turn are steadily shifted centrifugally during late L4, with new points added to maintain equal spacing (see panel B below).

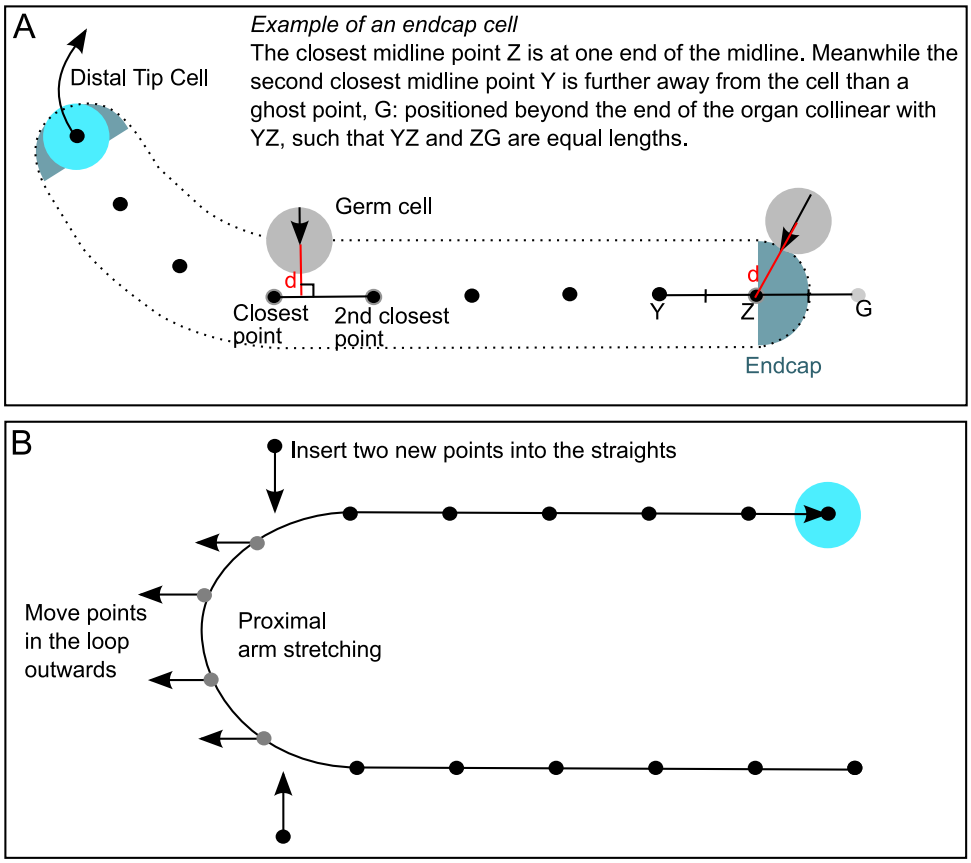

Boundary condition enforcement algorithm. (A) Indicates how germ cells are confined to the gonad, by correcting their positions relative to the DTC path. Cells in the endcaps are repositioned by being moved toward the end of the midline as required, generating a hemispherical cap. A dotted line in (A) indicates the shape of the resulting boundary condition. (B) Shows how the "stretching" of the gonad during late L4 is captured, by moving midline points in the turn, and inserting new points to maintain equal spacing.

3) Statechart Updates

The state of one of the 16 starting cells in our model is described by the chart below.

Only the initially active cell cycle phase may differ between starting cells; some may begin in G1, G2 or M rather than S phase.

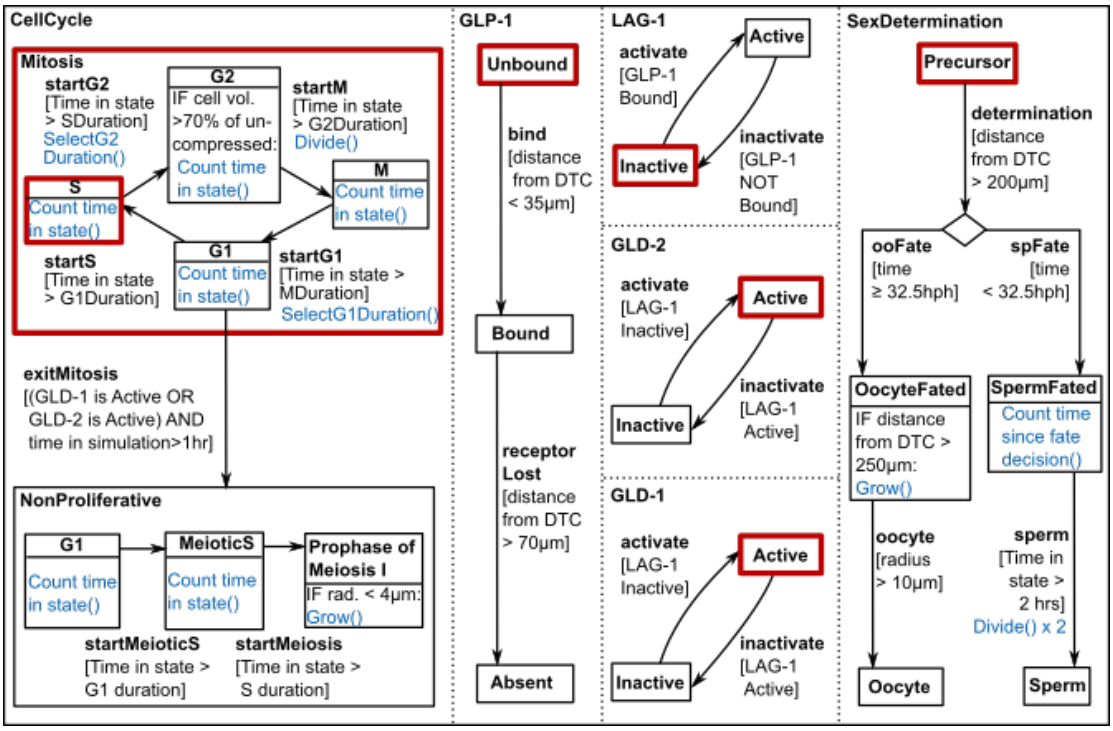

Initial cell state. Red = active.

A transition out of this active set of states occurs whenever one of the transition conditions in square brackets is met. So for instance, since all cells are initially within 35 μm of the DTC, the condition is met for GLP-1 to become bound immediately. GLP-1 binds, and as a result LAG-1 activates and GLD-1/2 inactivate:

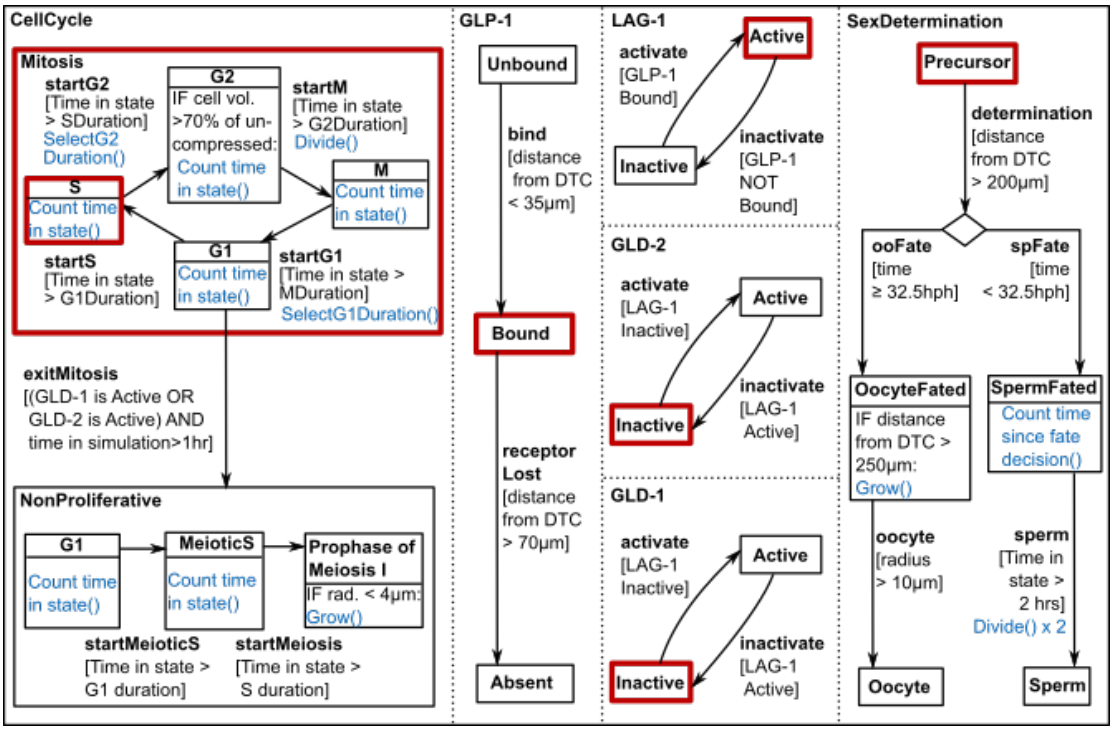

Cell state after one set of updates. GLP-1 binds, LAG-1 activates and GLD-1/2 inactivate.

When a cell moves further than 70 μm from the DTC, it meets the condition for GLP-1 to become *Absent*. As a result, LAG-1 becomes inactive and GLD-1/2 become active. There is no immediate effect on proliferative capacity unless the cell is also in the G1 state, as the transition arrow into *NonProliferative* comes from *G1* only:

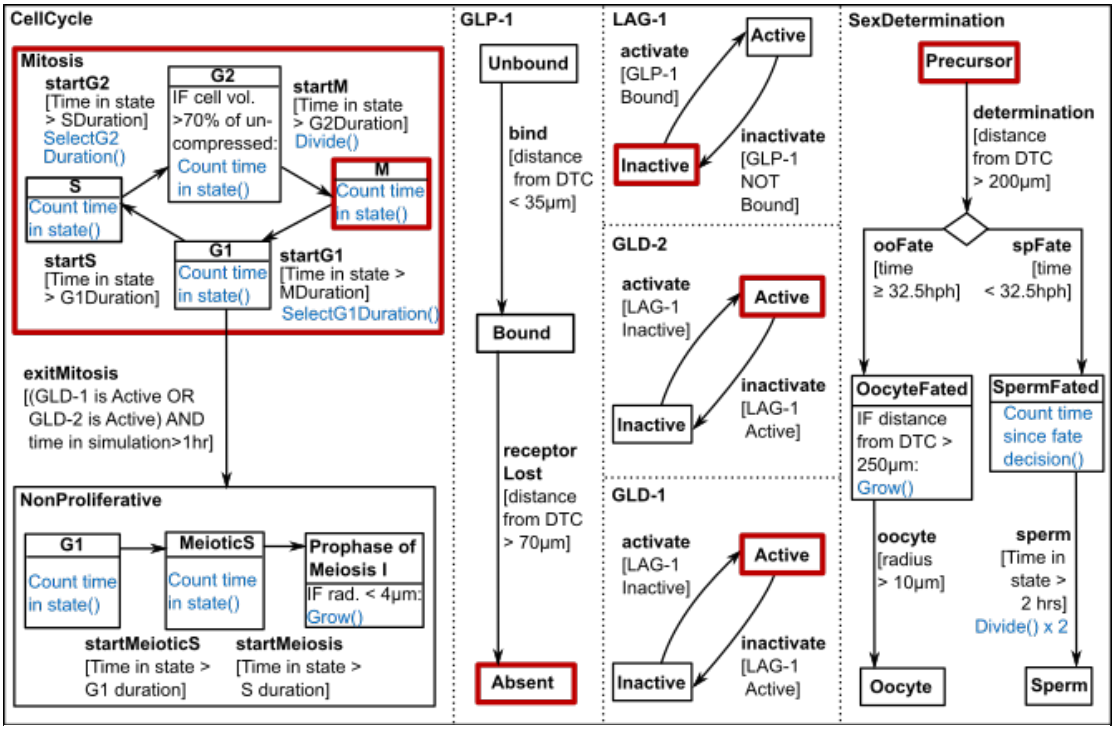

State in a cell >70µm from the DTC. GLP-1 becomes absent, LAG-1 inactivates and GLD-1/2 activate.

Subsequent changes in cell state follow similarly, occurring whenever a transition condition is met. Not all conditions are distance based; the sperm/oocyte fate decision depends on time post-hatching, the decision to exit proliferation depends on the cell cycle phase state of *Mitosis* as well as the states of GLD-1 and GLD-2, and the decision to advance to the next cell cycle phase depends on whether sufficient time has elapsed according to an internal counter. In addition, there are certain "actions" that are carried out while in a particular state (shown in blue). For instance, cells currently in *Prophase of Meiosis I* are instructed to grow, provided their current radius is < 4 μm.

Finally, cell movement and death are not part of the statechart model; they are handled separately in the mechanics simulation. Cell death is described in the main materials and methods.

4) Mechanical Feedback

As indicated in the statechart, proliferative cells count the amount of time they have spent in their current cell cycle phase, and move on to the next phase after a certain time delay has elapsed. This delay is determined on entry into the phase: for S and M phases the delay is fixed, for G1 and G2 it incorporates some randomness to avoid synchronisation (as described in the main materials and methods). In our model, this

counter temporarily pauses in G2 phase cells that are under "heavy compression", leading to a transient G2 arrest.

A cell is defined to be under "heavy compression" if its current compressed volume is less than 70% of its rest volume. The rest volume of a cell is simply the volume of a sphere with radius *r* equal to the cell radius:

$$V_{\text{Rest}} = \frac{4}{3}\pi r^3.$$

The compressed volume of a cell, meanwhile, is calculated by working out an *Effective Radius* ($R_{\text{Effective}}$) which takes into account the effect of neighbouring cells that overlap with the cell of interest (as in Dunn et al., 2013). Briefly, let:

$$R_{\text{Sum}} = \sum_{\text{Neighbors}} r - 0.5(r + r_{\text{Neighbor}} - d).$$

Where *d* is the cell separation. If the number of overlapping cells is less than 12 (the number of neighbours expected in a maximally efficient sphere packing), then a correction term is applied to take into account the fact that the cell has extra space available in certain directions:

$$R_{\text{Effective}} = \frac{R_{\text{Sum}} + N^* r}{12},$$

where

$$N^* = 12 - N_{\text{Neighbors}}.$$

Otherwise no such correction is needed:

$$R_{\text{Effective}} = \frac{R_{\text{Sum}}}{N_{\text{Neighbors}}}.$$

The final compressed cell volume is the volume of a sphere with radius equal to the Effective Radius:

$$V^* = \frac{4}{3}\pi \, {R_{\text{Effective}}}^3.$$

References

Dunn, S. J., Näthke, I. S., Osborne, J. M. (2013). Computational models reveal a passive mechanism for cell migration in the crypt. *PLOS One*. **8**, e80516.

Mirams, G. R., Arthurs, C. J., Bernabeu, M. O., Bordas, R., Cooper, J., Corrias, A., Davit, Y., Dunn, S. J., Fletcher, A. G., Harvey, D. G. et al. (2013). Chaste: An open source C++ library for computational physiology and biology. *PLOS Comput Biol*. **9**, e1002970.